Tanzania Journal of Science 48(3): 569-584, 2022
ISSN 0856-1761, e-ISSN 2507-7961

Modelling the Impacts of Immigrants on COVID 19 Transmission Dynamics with Control Measures

Alfred K. Hugo[1], Goodluck M. Mlay[2*] and Moses Baraka Kabigi[3]
[1]*Department of Mathematics and Statistics, University of Dodoma, P.O. Box 338, Dodoma, Tanzania*
[*2]*Department of Mathematics, University of Dar es Salaam, P.O. Box 35062, Dar es Salaam, Tanzania*
[3]*Ilonga Teachers College, P.O. Box 98, Kilosa, Morogoro, Tanzania*
[*]*Corresponding author, e-mail: goodluckmlay@gmail.com*
Received 23 Nov 2021, Revised 3 Aug 2022, Accepted 15 Aug 2022, Published Sep 2022
DOI: https://dx.doi.org/10.4314/tjs.v48i3.5

Abstract

The COVID-19 pandemic began in Wuhan City in the Hubei province of China in December 2019. The disease spread quickly in many countries around the world due to mobility of people from one location to another. As a result, a COVID-19 mathematical model with the impacts on immigrants was proposed to study its transmission dynamics and possible control measures. The reproduction number was determined by using the next-generation technique and found to be 0.636, indicating that the transmission could be minimized in the community if all immigrants were effectively controlled. The Pontryagin's Maximum Principle was applied in analysing control strategies which are screening of immigrants, provision of public education to raise community awareness, and treatment of infected individuals. The simulated results revealed that a combination of public education, screening of all immigrants, and treatment of infected individuals plays a significant role in reducing COVID-19 transmission in the community.

Keywords: COVID-19, Immigrants, Optimal control theory.

Introduction

The COVID-19 outbreak initially occurred in Wuhan City in Hubei province of China in December 2019. It quickly spread to numerous nations worldwide (Singh et al. 2020) and the World Health Organization (WHO) declared it a pandemic on March 11, 2020 (Adegboye et al. 2020). COVID-19 is transmitted by infected individuals through coughing or sneezing, whereby tiny droplets with viruses enter the mouth or the nose of a susceptible individual, causing an infection to occur. On the other hand, a susceptible individual may pick viruses from the surfaces contaminated by droplets from infected individuals (Seidu 2020). Fever or chills, cough, shortness of breath or difficulty breathing, fatigue, muscle or body aches, headache, loss of taste, sore throat, congestion or runny nose, vomiting, and sometimes diarrhoea are typical symptoms of COVID-19 (Adhikari et al. 2020, Jia et al. 2020, Mumbu and Hugo 2020). Currently, there is no proper treatment rather than the use of vaccines and traditional treatments. In addition, non-pharmaceutical interventions, such as the use of masks, hand washing, sanitizers, and other health care approaches play vital roles in the disease control.

During the COVID-19 pandemic, people travelled from one country to another for fear of disease contamination or other business reasons. Some countries around the world tightened restrictions on international arrivals

to slow the spread of the disease (Gwee et al. 2021). Indeed, COVID-19 has slowed economic growth, reduced the number of tourists, as well as technological transfers (Tchoumi et al. 2022). Some studies have been conducted on the transmission of COVID-19 in the presence of immigrants. Alfred et al. (2021) evaluated the impacts of immigrants in the context of Tanzania, where the output indicated that as the number of infected immigrants increases in relation to social interactions, it resulted in high transmission rate. Tchoumi et al. (2022) studied the impacts of infectious immigrants and discovered that increasing vaccination rates significantly reduced infections and transmissions regardless of the number of deaths that occurred.

On the other hand, Xing et al. (2020) used the SEIR model to study the impacts of population migration around the Spring Festival on the spread of COVID-19 in China's Guangdong and Hunan provinces; discovered that immigrants contributed significantly to COVID-19 transmission. Furthermore, Marouf (2021) reported that COVID-19 has rapidly spread through immigration in the United States, where the government decided to establish a medical tracking system for all immigrants to reduce transmission. Additionally, the World Health Organization (2021) classified national COVID-19 adaptation policies; public health policies on migrants and refugees access to health care and migrant policy response to COVID-19 for foreigners within national borders for the purpose of reducing the transmission. On other hand, immigration strategies were analysed to justify the causes of the disease spread in the community (Kassa et al. 2020).

According to Lee et al. (2020), Singapore utilizes a range of techniques to minimize disease spread including precautionary measures such as restricting large gatherings and conducting temperature check-ups for community members in public services. Rahman and Kuddus (2021) analysed control measures against COVID-19 transmission in Ghana and found that people should use hand sanitizers, wash their hands regularly and practice social distance. In China, Adhikari et al. (2020) investigated the epidemiology, causes, clinical diagnosis, prevention and control of COVID-19 where preventive strategies could workout in lowering the transmission in community. Jia et al. (2020) analysed the effects of home quarantine measures practised in China. Furthermore, Singh et al. (2020), and Ivorra et al. (2020) studied the COVID-19 in India using the standard SEQIR model from the stochastic dynamics method, examining the impacts of quarantine and social isolation as proposed management strategies.

In controlling the transmission, it was argued that the government should expand the healthcare facilities (Tarimo and Wu 2020) including tracking of the immigrants. In addition, all travellers should seek medical attention and disclose their trip history to the doctors (Kucharski et al. 2020).

The particular study is sought to create a mathematical model accounting for the impacts of immigration toward the transmission of COVID 19. It also designed to assess the effectiveness of COVID-19 control techniques which are screening of immigrants, provisional public education to raise community awareness, and treatment of infected individuals.

Materials and Methods

In this section, a deterministic mathematical model of human population with the effects of immigrants has been developed. The modelled population is divided into four subclasses: susceptible population $S(t)$, that includes all healthy individuals who are likely to become infected when interacting with infectious ones, $E(t)$ represents exposed individuals who may have been infected but are not infectious, whereas individuals who developed clinical symptoms and can transmit disease to others are represented by $I(t)$. The symbol $R(t)$, on the other hand, represents all individuals who gain immunity through supportive services or treatment, either by natural means or by being admitted to hospital. The immigrant aspects are introduced to the susceptible class for analysing their effects on disease

transmission and the following parameters are taken into account in the model formulation:

i The rate at which the human population recruited in susceptible group is expressed as $\prod = p\left(1-\pi_1-\pi_2\right)$, where π_i for $i=1,2$ are the rates of immigrants which enter into exposed class $E(t)$ and infected class $I(t)$, respectively and p representing recruitment rate.

ii The disease transmission occurs in the susceptible population through direct contact with an infected individual at the rate of α.

iii The infected individuals are transferred to the recovered class at the rate of τ and those who gain immunity join the class of susceptible by the rate η.

iv The population decreases through the natural mortality rate μ as well as disease induced death rate of m.

Putting into consideration the parameters and the state variables the following model equations were formulated:

$$\begin{aligned}
\frac{dS}{dt} &= p\left[1-\left(\pi_1+\pi_2\right)\right]-\beta SI+\eta R-\mu S\\
\frac{dE}{dt} &= \beta SI+p\pi_1-\left(\alpha+\mu\right)E\\
\frac{dI}{dt} &= \alpha E+p\pi_2-\left(m+\mu+\tau\right)I\\
\frac{dR}{dt} &= \tau I-\left(\mu+\eta\right)R
\end{aligned} \tag{1}$$

such that

$S(t)>0, E(t)>0, I(t)>0, R(t)>0$.

Invariant region

Since the model involves people, all parameters must therefore be in an invariable positive region for all $t \geq 0$. Addition of all equations in system (1) and further simplification results to;

$$\frac{dN}{dt} = p-\mu N-mI \tag{2}$$

Suppose $m=0$ then (2) becomes;

$$\frac{dN}{dt} \leq p-\mu N \tag{3}$$

Applying Birkhoff and Rota (1982) theorem equation (3) becomes

$$N \leq \frac{p}{\mu}-\left(\frac{p}{\mu}-N_0\right)e^{-\mu t} \tag{4}$$

Thus, as $t \to \infty$ then (4) gives $N=\frac{p}{\mu}$.

Hence, $\Omega=\left\{S,E,I,R \in \mathbf{R}_+^4 : N \leq \frac{p}{\mu}\right\}$.

Therefore, the feasible region for the system (1) in $\mathbf{R}_+^4$ is well-posed.

Positivity of solution

Lemma 1. *Let* $\left\{N(0)>0; S>0, E(0), I(0), R(0) \geq 0\right\} \in \Omega$. *Then the set of solutions of the model system of equations (1)* $\left\{S,E,I,R,N\right\}$ *are positive for* $\forall t \geq 0$.

Proof. From the system (1), the first equation gives

$$\frac{dS}{dt} \geq p[1-(\pi_1+\pi_2)]-\mu S \tag{5}$$

Integrating equation (5) and applying the initial conditions yields;

$$S \leq \frac{p(1-(\pi_1+\pi_2))}{\mu}-\left(\frac{p(1-(\pi_1+\pi_2))}{\mu}-S_0\right)e^{-\mu t} \tag{6}$$

From equation (6) it follows that as $t \to \infty$, then $S=\frac{p(1-(\pi_1+\pi_2))}{\mu}$ (7)

A similar approach can be applied in the rest of the model equations of the system (1) for all $t > 0$. Therefore, $\{S(0) \geq 0, E(0) \geq 0, I(0) \geq 0, R(0) \geq 0\} \quad \forall t \geq 0$. □

Steady-state

The disease-free equilibrium (DFE) point of the system of equations in (1) is obtained by setting the right-hand side of each equation equal to zero, resulting in

$$E_0 = \left(S^*, E^*, I^*, R^*\right) = \left(\frac{p[1-(\pi_1+\pi_2)]}{\mu}, 0, 0, 0\right). \tag{8}$$

Basic reproduction number

In mathematical epidemiology, the basic reproduction number R_0 refers to the average number of secondary infected individuals produced during the life of a single primary infected individual. The R_0 for this study was determined by using Next-generation technique as applied by Van den Driessche and Watmough (2002). For this particular model, the R_0 is given as:

$$R_0 = \frac{\alpha\beta\ \Pi}{\mu(\alpha+\mu)(m+\mu+\tau)}. \tag{9}$$

Stability analysis of DFE

The local stability of E_0 is evaluated as;

$$J_{E_0} = \frac{\partial(f_1, f_2, f_3, f_4)}{\partial(S, E, I, R)} = \begin{bmatrix} -\mu & 0 & \frac{-\beta\ \Pi}{\mu} & \eta \\ 0 & -(\alpha+\mu) & \frac{\beta\Pi}{\mu} & 0 \\ 0 & \alpha & -(m+\mu+\tau) & 0 \\ 0 & 0 & \tau & -(\eta+\mu) \end{bmatrix}. \tag{10}$$

Matrix (10) gives eigenvalues of $\lambda_1 = -\mu, \lambda_2 = -(\eta+\mu)$ and the other two eigenvalues are the positive solution of

$$f(\lambda) = \lambda^2 + A\lambda + B, \tag{11}$$

where $A = [(\alpha+\mu)+(m+\mu+\tau)]$ and $B = (\alpha+\mu)(m+\mu+\tau) - \frac{\Pi\alpha\beta}{\mu}$.

Applying the Routh-Hurwitz technique as, $A > 0, AB > 0$ and since $A > 0$ then $B > 0$ it follows that

$(\alpha+\mu)(m+\mu+\tau) - \frac{\Pi\alpha\beta}{\mu} > 0$, implying that $\frac{\Pi\alpha\beta}{\mu(\alpha+\mu)(m+\mu+\tau)} < 1$. That is to say $R_0 < 1$.

Hence, Theorem 1 summarizes the results.

Theorem 1*: If $R_0 < 1$ then the disease-free equilibrium is locally asymptotically stable otherwise if $R_0 > 1$ it is unstable.*

Global stability of E_0

We examine DFE's global stability as

$$\begin{cases} \dfrac{dX_s}{dt} = A(X_s, X_i) \\ \dfrac{dX_i}{dt} = B(X_s, X_i), \qquad B(X_s, 0) = 0 \end{cases} \tag{12}$$

where:

$$X_S = (S, R), X_I = (E, I) \text{ and } E_0 = \left(\frac{\Pi}{\mu}, 0, 0, 0\right).$$

X^* is globally asymptotically stable (GAS) if it is satisfying the following two conditions:

$$\begin{cases} 1.\ \dfrac{dX_s}{dt} = A(X_s, 0), \\ 2.\ \dfrac{dX_i}{dt} = B(X_s, X_i) = EX_i - \tilde{B}(X_s, X_i). \end{cases} \tag{13}$$

This implies that $\tilde{B}(X_S, X_I) \geq 0$ for $(X_S, X_I) \in \phi$ where E is a Metzler Matrix and ϕ is the region of the model system (1) which is GAS if two conditions in (13) satisfy the Theorem 2.

Theorem 2: *The disease-free equilibrium point* $\left(\dfrac{\Pi}{\mu}, 0, 0, 0\right)$ *of the model system (1) is GAS if* $R_0 < 1$ *withholding conditions 1 and 2 in (13) otherwise it is unstable.*

Proof. Condition 1 in (13) is proved as follows:

Let

$$A(X_S, X_i) = \begin{bmatrix} \Pi - \beta IS + \eta R - \mu S \\ \tau I - (\eta + \mu) R \end{bmatrix} \text{ and } A(X_S, O) = \begin{bmatrix} \Pi - \mu S \\ 0 \end{bmatrix},$$

which gives $S(t) = \dfrac{\Pi}{\mu} + Ae^{-\mu t}$.

Then at $t = 0$, $S(t) = \dfrac{\Pi}{\mu} + \left(S(0) - \dfrac{\Pi}{\mu}\right)e^{-\mu t}$. Furthermore, as $t \to \infty$ then the solution becomes $S(t) \to \dfrac{\Pi}{\mu}$ implying that E_0 is global asymptotically stable.

Model (1) has to satisfy condition 2 as

$$B(X_s, X_i) = EX_i - \tilde{B}(X_s, X_i) = \begin{pmatrix} \beta I(S_0 - S) - p\pi_1 \\ p\pi_2 \end{pmatrix}.$$

Stability of Metzler matrix E by Routh-Hurwitz technique

$$\begin{vmatrix} -(\alpha + \mu) - \lambda & \dfrac{\beta\Pi}{\mu} \\ \alpha & -(m + \mu + \tau) - \lambda \end{vmatrix} = 0 \tag{14}$$

Thus, the equation generated in (14) has the same characteristics as equation (10), hence, E is a Metzler matrix and stable when $R_0 < 1$. □

Existence and stability for E^*

The endemic equilibrium point is denoted by E^* obtained as

$S^* = \frac{\Pi(\eta+\mu)+\eta p\tau I^*}{(\eta+\mu)\left(\beta I^*+\mu\right)}$, $R^* = \frac{\tau I^*}{\eta+\mu}$ and

$$E^* = \frac{\beta I^*\left((\eta+\mu)\Pi+\eta p\tau I^*\right)+p\pi_1\left[(\eta+\mu)\beta I^*+\mu(\eta+\mu)\right]}{(\alpha+\mu)\left[(\eta+\mu)\beta I^*+\mu(\eta+\mu)\right]}$$

and I^* is the positive root of

$$A\left(I^*\right)^2+BI^*+C=0, \tag{15}$$

where,

$$A=\alpha\beta\left[\eta\tau-\frac{\Pi\beta(\eta+\mu)}{R_o\mu}\right], C=\mu(\eta+\mu)\left[\alpha p\pi_1+p\pi_2(\alpha+\mu)\right],$$

$$B=\alpha\beta p\left(1-(\pi_1+\pi_2)\right)\left((\eta+\mu)-\frac{1}{R_o}\right)+p\pi_1\beta+p\pi_2\beta(\alpha+\mu)(\eta+\mu).$$

Local stability of endemic equilibrium point, E_1

Local stability of endemic equilibrium points near $R_0=1$ is analysed by using the centre of manifold Theorem as it is presented in Mukandavire et al. (2009). This method is implemented by renaming the state variables of the COVID-19 model (1) as to

$S=x_1,\ \mathrm{E}=x_2,\ \mathrm{I}=x_3, R=x_4$ where

$X_i=\left(x_1,\ x_2,\ x_3,\ x_4\right)^T$,

$\frac{dX_i}{dt}=F(X_i),\quad F=(f_1,\ f_2,\ f_3,\ f_4)^T$, where $(.)^T$ is a matrix transpose.

Thus,

$$\frac{dx_1}{dt}=p\left[1-(\pi_1+\pi_2)\right]-\beta x_1x_3+\eta x_4-\mu x_1,$$

$$\frac{dx_2}{dt}=\beta x_1x_3+p\pi_1-(\alpha+\mu)x_2,$$

$$\frac{dx_3}{dt}=\alpha x_2+p\pi_2-(m+\mu+\tau)x_3,$$

$$\frac{dx_4}{dt}=\tau x_3-(\mu+\eta)x_4. \tag{16}$$

The Jacobian matrix at DFE is

$$A=\begin{bmatrix} -\mu & 0 & \dfrac{-\Pi\beta}{\mu} & \eta \\ 0 & -(\alpha+\mu) & \dfrac{\Pi\beta}{\mu} & 0 \\ 0 & \alpha & -(m+\mu+\tau) & 0 \\ 0 & 0 & \tau & -(\eta+\mu) \end{bmatrix}. \tag{17}$$

Theorem 3. *Consider the following general system of ordinary differential equations with a parameter* ϕ*, then*

$$\frac{dx}{dt}=f(x,\phi),\ f:\Re^n\times\Re\to\Re^n \text{ and } f\in\Re^2\left(\Re^n\times\Re\right), \tag{18}$$

where 0 is an equilibrium point of the system, that is, $f(0,\phi)\equiv 0\ \forall\phi$ *and let assume that.*

1. $A=D_X f(0,0)=\left[\dfrac{\partial f_i}{\partial x_j}(0,0)\right]$ *is the linearization matrix of the system around the equilibrium 0 with* ϕ *evaluated at 0;*
2. *Zero is a simple eigenvalue of* A *and all other eigenvalues* A *have negative real parts;*
3. *Matrix* A *has a right eigenvector* w *and a left eigenvector* v *corresponding to the zero eigenvalue.*

Let f_k *be the* k^{th} *component of* f *and*

$$a=\sum_{k,i,j=1}^{n} v_k w_i w_j \frac{\partial^2 f_k}{\partial x_i \partial x_j}(0,0),\quad b=\sum_{k,i=1}^{n} v_k w_i \frac{\partial^2 f_k}{\partial x_i \partial \phi}(0,0). \tag{19}$$

The local dynamics of the system (19) around 0 are determined by the signs of a *and* b.

(i) $a>0, b>0$. *When* $\phi<0$ *with* $|\phi|<<1$, *0 is locally asymptotically stable, and there exists a positive unstable equilibrium; when* $0<\phi<<1$ *0 is unstable and there exists a negative and locally asymptotically stable equilibrium;*

(ii) $a<0, b<0$. *When* $\phi<0$ *with* $|\phi|<<1$, *0 is unstable; when* $0<\phi<<1$, *0 is locally asymptotically stable, and there exists a positive unstable equilibrium;*

(iii) $a>0, b<0$. *When* $\phi<0$ *with* $|\phi|<<1$, *0 is unstable, and there exists a locally asymptotically stable negative equilibrium; when* $0<\phi<<1$, *0 is stable, and a positive unstable equilibrium appears;*

(iv) $a<0, b>0$ *When* ϕ *changes from negative to positive, 0 changes its stability from stable to unstable. Correspondingly, a negative unstable equilibrium becomes positive and locally asymptotically stable. Particularly if* $a>0$ *and* $b>0$, *then a backward bifurcation occurs at* $\phi=0$.

Take β^* as a bifurcation parameter, consider

$$R_0 = 1 = \frac{\alpha\beta p[1-(\pi_1+\pi_2)]}{\mu(\alpha+\mu)(m+\mu+\tau)}.$$

By using $\beta = \beta^*$ and making β^*

$$\beta^* = \frac{\mu(\alpha+\mu)(m+\mu+\tau)}{\alpha p[1-(\pi_1+\pi_2)]}. \tag{20}$$

Thus, substituting (20) into (17) gives

$$J_{\beta^*} = \begin{bmatrix} -\mu & 0 & \frac{-(\alpha+\mu)(m+\mu+\tau)}{\alpha} & \eta \\ 0 & -(\alpha+\mu) & \frac{(\alpha+\mu)(m+\mu+\tau)}{\alpha} & 0 \\ 0 & \alpha & -(m+\mu+\tau) & 0 \\ 0 & 0 & \tau & -(\eta+\mu) \end{bmatrix}. \tag{21}$$

Then, the eigenvalues of (21) are $\{0, -\mu, -(\eta+\mu), -(m+\mu+\tau)\}$ thus zero is an eigenvalue of J_{β^*}. Therefore, Theorem 3 holds under condition 2.

The associated eigenvectors corresponding with zero eigenvalues of (21) are

$$w_1 = \frac{\eta}{\mu} - \frac{(\eta+\mu)(\alpha+\mu)(m+\mu+\tau)}{\alpha\mu\tau}, w_2 = \frac{(\eta+\mu)(m+\mu+\tau)}{\alpha\tau}, w_3 = \frac{(\eta+\mu)}{\tau}, w_4 = 1.$$

From (21) the eigenvectors of transpose the matrix (21) associated with zero eigenvalues are given as

$$v_1 = 0, v_2 = \frac{\alpha}{\alpha+\mu}, v_3 = 1, v_4 = 0.$$

Computational of a and b.

The associated non-zero second-order partial derivative of (16) at disease-free equilibrium and β^* are given by.

$$a = \sum_{k,i,j=1}^{n} v_k w_i w_j \frac{\partial^2 f_k}{\partial x_i \partial x_j}(x_0, 0), \quad \frac{\partial^2 f_2}{\partial x_1 \partial x_3} = \frac{\partial^2 f_2}{\partial x_3 \partial x_1} = \frac{\beta}{N},$$

$$a = v_2 w_1 w_3 \frac{\partial^2 f_2}{\partial x_1 dx_3} + v_2 w_3 w_1 \frac{\partial^2 f_2}{\partial x_3 \partial x_1}.$$

Then,

$$a = \left[\frac{\alpha\eta\tau(\eta+\mu)(m+\mu+\tau) - (\alpha+\mu)\left((\eta+\mu)(m+\mu+\tau)\right)^2}{\mu\tau^2\alpha(\alpha+\mu)} \right].$$

If $\alpha\eta\tau(\eta+\mu)(m+\mu+\tau) < (\alpha+\mu)\left((\eta+\mu)(m+\mu+\tau)\right)^2$,

then $a < 0$, otherwise $a > 0$.

Calculation for b

$$b=\sum_{k,i=1}^{n} v_k w_i \frac{\partial^2 f_k}{\partial x_i \partial \beta^*}(x_0,0) \quad b=\frac{(\eta+\mu)(p[1-(\pi_1+\pi_2)])}{\mu\tau}.$$

This implies that $\frac{(\eta+\mu)\left(p\left[1-(\pi_1+\pi_2)\right]\right)}{\mu\tau}>0$ and hence $b>0$.

This is clear that $a<0$ and $b>0$ as per the conditions stated. The analysis is therefore supported by Figure 1.

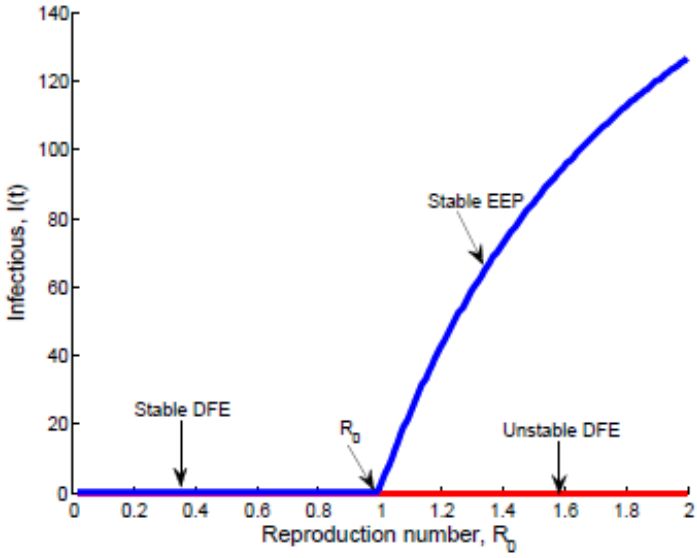

Figure 1: The bifurcation analysis of the model.

Application of optimal control

In this section, Pontryagin's Maximum Principles are applied to model (1) to determine the necessary conditions for the existence of optimal control of COVID-19. This aims to reduce the number of people in the community who might have COVID-19 by implementing three-time dependent control strategies. The first control, $u_1(t)$, is associated with screening and testing of immigrants, while the second control, $u_2(t)$, is associated with raising awareness through public education campaigns, and the third control, $u_3(t)$, is associated with prevention through treatment of infected individuals.

The system of the model (1) becomes

$$\begin{cases} \dfrac{dS}{dt} = p\left[1-\left(1-u_1\right)\left(\pi_1+\pi_2\right)\right]-\left(1-u_2\right)\beta SI+\eta R-\mu S, \\ \dfrac{dE}{dt} = \left(1-u_2\right)\beta SI+\left(1-u_1\right)p\pi_1-\left(\alpha+\mu\right)E, \\ \dfrac{dI}{dt} = \alpha E+\left(1-u_1\right)p\pi_2-\left(m+\mu\right)I-\left(\tau+u_3\right)I, \\ \dfrac{dR}{dt} = \left(\tau+u_3\right)I-\left(\mu+\eta\right)R, \end{cases} \tag{22}$$

with $S(0)\geq 0,\ E(0)\geq 0,\ I(0)\geq 0,\ R(0)\geq 0$. Furthermore, control functions $u_1\left(t\right)$, $u_2\left(t\right)$ and $u_3\left(t\right)$ are assumed to be Lebesgue integrable functions at $\left[0,t_f\right]$.

$U=u_i:0\leq u_i\leq 1,\text{for } i=\ 1,\ 2,\ 3$. Thus, the objective functional is presented as;

$$J(u_1,u_2,u_3)=\int_0^{t_f}\left(A_1E+A_2I+B_1\frac{u_1^2}{2}+B_2\frac{u_2^2}{2}+B_3\frac{u_3^2}{2}\right)dt, \tag{23}$$

where the constants A_i and B_j for $i=1,2,3$ and $j=1,2,3$ taken as positive weights. Further $\frac{B_1u_1^2}{2}$ characterizes the effort of cost control on screening of immigrants, $\frac{B_2u_2^2}{2}$ represents the cost associated with implementing public education campaigns, and $\frac{B_3u_3^2}{2}$ represents the costs associated with the treatment of infected individuals. A quadratic function that meets the optimality conditions is considered to minimize $u_1(t)$, $u_2(t)$ and $u_3(t)$ determine optimal control u_1^* u_2^* and u_3^* such that

$$J\left(u_{11}^*,u_2^*,u_3^*\right)=\min\left\{J\left(u_1,u_2,u_3\right)\mid u_1,u_2,u_3\in\Omega\right\},$$

where

$\Omega=\left\{\left(u_1,u_2,u_3\right)\right.$ such that u_1,u_2,u_3 are measurable with $0\leq u_1\leq 1, 0\leq u_2\leq 1$ and $0\leq u_1\leq 1$ $0\leq t\leq t_f$. The Hamiltonian function (H) is therefore defined as:

$$H(S,E,I,R)=A_1E+A_2I+\sum_{i=1}^{3}\frac{B_iu_i^2}{2}+\lambda_1\frac{dS}{dt}+\lambda_2\frac{dE}{dt}+\lambda_3\frac{dI}{dt}+\lambda_4\frac{dR}{dt}, \tag{24}$$

where: $\lambda_i,\ i=1,2,3,4$ are adjoint variables (co-state variables).

Optimal control existence

The existence of control is evaluated through the results obtained by Fleming and Rishel (1975) through the following theorem.

Theorem 4. *Let the optimal control problem that minimizes the objective function J be defined over a time [0, T]. If the function is defined on a set of bounded and lebesgue measurable control and subjected to the dynamic constraint of some state equations, then there exists an optimal solution such that* $J\left(u^*\right)=\min_u u$ *provided that the following conditions hold:*

(i) The control set is convex and closed.

(ii) *The right-hand side of the state system is bounded by a linear function in the state and control variable.*

(iii) *The state variables used in the system (1), together with their control variables are not empty.*

(iv) *There exist some constants* $x_1,\ x_2 > 0$ *and* $y_1 > 0$, *for which the integrand of the objective function is convex and satisfies the condition:*

$$J(u) = x_1\left(\sum_{i=1}^{n}|u_i|^2\right)^{\frac{y_1}{2}} - x_2 .$$

The proof of Theorem 4 was found in the book of Fleming and Rishel (1975) entitled Deterministic and Stochastic optimal control and Lenhart and Workman (2007). Conversely, for the analysis of a particular paper, the conditions that guarantee the existence of an optimal solution for the objective functional are verified. Consider an optimal control, which is subject to the state constraint given by the system;

1. By definition, the control variables $u_1,\ u_2, u_3$ are convex and closed.
2. The solutions of the state system are bounded since the state functions are linear about the control variables. Hence, the second condition is satisfied.
3. The state and our corresponding set of control variables u in the system (1) are presumed bounded and not empty.
4. As the result of boundedness, thus $a_1,\ a_2 > 0$ and $B_1 > 0$, for which the integrant of the objective functional is convex and satisfies

$$A_1E + A_2I + \sum_{i=1}^{3}\frac{B_i u_i^2}{2} \geq a_1\left(\sum_{i=1}^{n}|u_i|^2\right)^{\frac{y_1}{2}} - x_2 .$$

Therefore, it is worth it to be concluded that there exists an optimal solution that lies between 0 and 1 that minimizes the objective function.

Necessary optimality conditions

The optimality condition of the solution of the model is determined based on the following theorem.

Theorem 5. *Let* u_i *be the set of optimal control and* X_i *be the corresponding solution of the set of equations that minimizes the objective function J over the set of controls, then there exist* λ_j *adjoint variables such that the optimality system is*

$$\begin{cases} \dfrac{d\lambda_j}{dt} = -\dfrac{\partial H}{dX}, \\ \lambda_j(t_f) = 0, \\ \dfrac{\partial H}{\partial u} = 0. \end{cases}$$

For the optimal controls u_1^* u_2^* and u_3^* to minimize $J(u_1, u_2, u_3)$ over Ω, then there exist adjoint variables $\lambda_1, \lambda_2, \lambda_3$ and λ_4 satisfying;

(i) Adjoint equation

$$\frac{-d\lambda_j}{dt} = \frac{\partial H}{\partial j}, \quad (25)$$

where $j = S, E, I, R$.

(ii) Transversality conditions *(*final time) $\lambda_i(f_t) = 0,\ i = 1, 2, 3, 4$.

(iii) Optimality condition $\dfrac{\partial H}{\partial u_i} = 0$.

Characteristics of optimal controls u_1^*, u_2^* and u_3^* are based on the following conditions:

$$\frac{\partial H}{\partial u_1} = 0, \frac{\partial H}{\partial u_2} = 0 \text{ and } \frac{\partial H}{\partial u_3} = 0$$

subject to the constrains

$0 \leq u_1 \leq u_{1\max}, 0 \leq u_2 \leq u_{2\max}$ and $0 \leq u_3 \leq u_{3\max}$

where;

$$
\begin{aligned}
0 &= \frac{\partial H}{\partial u_1} = B_1 u_1 - \lambda_1^* \left(\pi_1 + \pi_2\right) p - \lambda_2^* p \pi_1 - \lambda_3^* p \pi_2 \\
0 &= \frac{\partial H}{\partial u_2} = B_2 u_2 + \lambda_1^* \beta S I - \lambda_2^* \beta S I \\
0 &= \frac{\partial H}{\partial u_3} = B_3 u_3 - \lambda_3^* I + \lambda_4^* I.
\end{aligned} \tag{26}
$$

$$
u_1^* = \frac{p\left(\pi_1\left(\lambda_2^* - \lambda_1^*\right) + \pi_2\left(\lambda_3^* - \lambda_1^*\right)\right)}{B_1}, u_2^* = \frac{\beta S^* I^* \left(\lambda_2^* - \lambda_1^*\right)}{B_2}
$$

and.

$$
u_3^* = \frac{I^* \left(\lambda_3^* - \lambda_4^*\right)}{B_3}
$$

$$
u_i^* = \begin{cases} 0 \text{ If } \omega_i^* \le 0 \\ \psi_i^* \text{ If } 0 < \omega_i^* < 1 \\ 1 \text{ If } \omega_i^* \ge 0 \end{cases}
$$

The controls are further presented as , for $i = 1, 2, 3$

where;

$$
\omega_1^* = \frac{p\left(\pi_1\left(\lambda_2^* - \lambda_1^*\right) + \pi_2\left(\lambda_3^* - \lambda_1^*\right)\right)}{B_1}, \omega_2^* = \frac{\beta S^* I^* \left(\lambda_2^* - \lambda_1^*\right)}{B_2}, \omega_3^* = \frac{I^* \left(\lambda_3^* - \lambda_4^*\right)}{B_3}.
$$

Then, the solution is characterized as

$$
u_1^* = \max\left\{0, \min\left(1, \frac{p\left(\pi_1\left(\lambda_2^* - \lambda_1^*\right) + \pi_2\left(\lambda_3^* - \lambda_1^*\right)\right)}{B_1}\right)\right\},
$$

$$
u_2^* = \max\left\{0, \min\left(1, \frac{\beta S^* I^* \left(\lambda_2^* - \lambda_1^*\right)}{B_2}\right)\right\}, \quad u_3^* = \max\left\{0, \min\left(1, \frac{I^* \left(\lambda_3^* - \lambda_4^*\right)}{B_3}\right)\right\}.
$$

Furthermore, the adjoint equations are given by

$$
\begin{aligned}
-\frac{\partial \lambda_1}{\partial t} &= \frac{\partial H}{\partial S} = \frac{\beta I \left(1 - u_2\right)\left(\lambda_1^* - \lambda_2^*\right)}{N} + \mu \lambda_1^*, \\
-\frac{\partial \lambda_2}{\partial t} &= \frac{\partial H}{\partial E} = \alpha\left(\lambda_2^* - \lambda_3^*\right) + \mu \lambda_2^* - A_1, \\
-\frac{\partial \lambda_3}{\partial t} &= \frac{\partial H}{\partial I} = \frac{\beta S \left(1 - u_2\right)\left(\lambda_1^* - \lambda_2^*\right)}{N} + \left(\tau + u_3\right)\left(\lambda_3^* - \lambda_4^*\right) + \lambda_3^* (m + \mu) - A_2, \\
-\frac{\partial \lambda_2}{\partial t} &= \frac{\partial H}{\partial R} = \eta\left(\lambda_4^* - \lambda_1^*\right) + \mu \lambda_4^*.
\end{aligned} \tag{27}
$$

Results and Discussions

In this section, numerical computations were performed to determine the best COVID-19 control strategy. To assess the impacts of control strategies, a numerical simulation was run with different parameters derived from various literature reviews based on disease dynamics. The initial and parameter values used in simulations include $S(t) = 55,000,000$, $E(t) = 4,000,000$, $I(t) = 509$, $R(t) = 183$, $\alpha = 0.02857$, $\beta = 0.5944$, $p = 1000000$ (Mumbu and Hugo 2020) and $\mu = 0.00875, \tau = 0.125$ (Adegboye et al. 2020), while $\pi_2 = 0.002$, $\pi_1 = 0.002$, $m = 0.0413$, $\eta = 0.36$ were assumed based on dynamics of the disease. Numerically, the simulations of the control strategies are therefore presented in Figure 2 to Figure 5.

Strategy 1: Effects of screening of immigrants, public education, and treatment of infected individuals

Figure 2 shows that the spread of COVID-19 has been restricted since day one, with the exposed population decreasing while the susceptible population grows, indicating that COVID-19 will be controlled in the community.

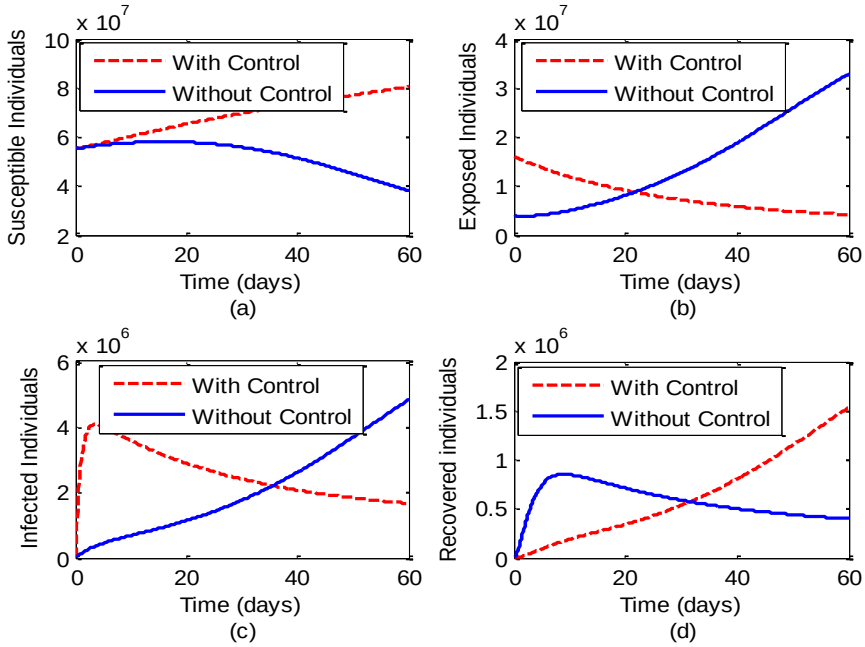

Figure 2: Effects of screening of immigrants, community education, and treatment of infected individuals.

Strategy 2: Effects of public education on the community and screening of immigrants

Figure 3 depicts the impacts of a public education campaign combined with a screening of the immigrant population. The data reveal that the number of infected people has decreased considerably, indicating a positive trend in reducing COVID-19 transmission in the community.

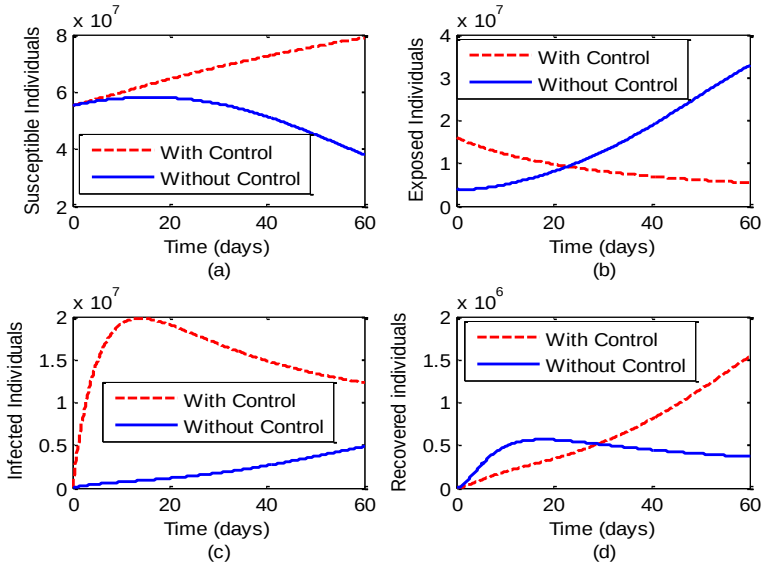

Figure 3: The effects of public education on the community and screening of immigrants.

Strategy 3: Effects of treatment of infected individuals and screening of immigrants

Figure 4 depicts the impacts of treatment and screening of immigrants, indicating that the infected class has decreased considerably, indicating that more individuals may recover and re-join the vulnerable class.

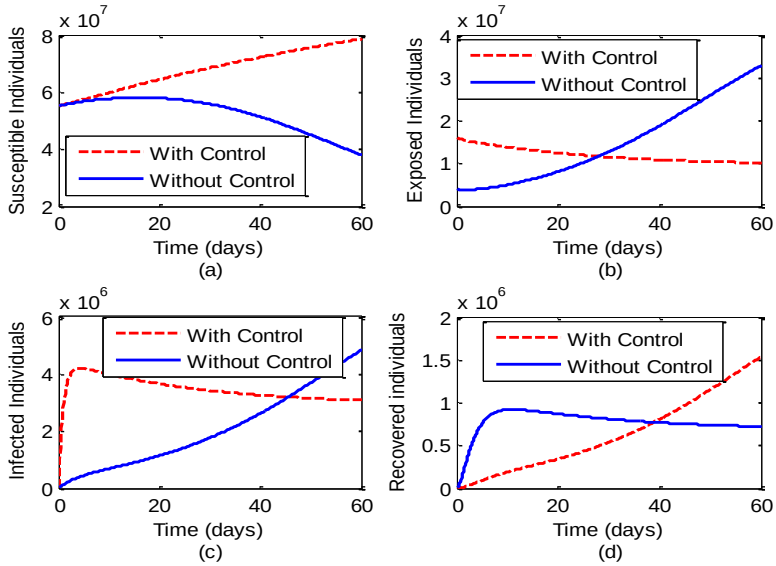

Figure 4: The effects of treatment of infected individuals and screening of immigrants.

Strategy 4: Effects of public education campaigns and treatment of infected individuals

The findings indicated that public education and treatment made a significant contribution to preventing disease transmission in the community, as shown in Figure 5. As a result, COVID-19 transmission is expected to decline, resulting in a reduction in the number of infected individuals.

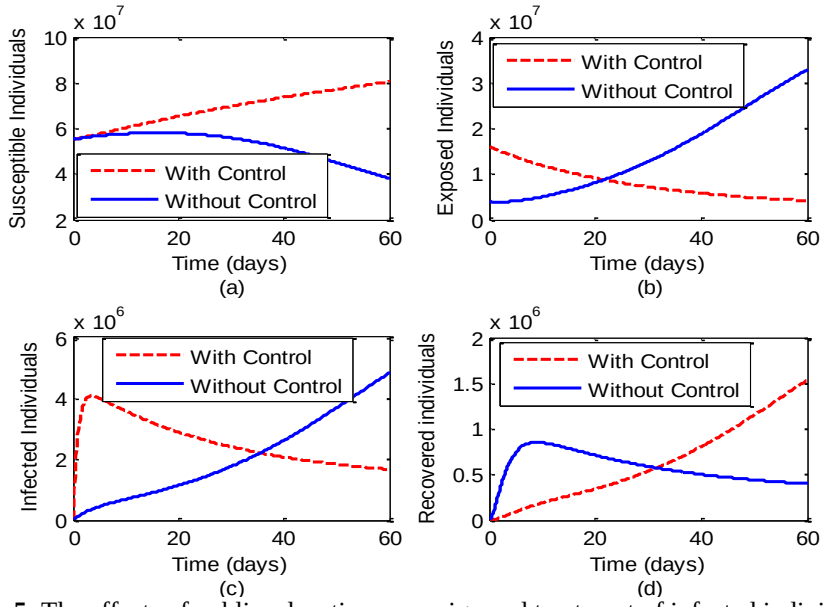

Figure 5: The effects of public education campaign and treatment of infected individuals.

Conclusion

In this paper, a non-linear mathematical model of COVID-19 with four compartments; susceptible, exposed, infectious, and recovered, has been proposed and studied. Theoretical and numerical analyses were carried out and the dynamical behaviour of the system was found to be mathematically well-posed. Reproduction number was computed by using the next-generation matrix method and through applying interventions its numerical value was 0.6365 showing that the COVID-19 can be controlled in the community as the members apply effective control measures. The Pontragin's Maximum Principle was employed to evaluate necessary conditions that an optimal control and corresponding state must satisfy. The results from simulations showed that applications of all control strategies (screening of immigrants, community education campaigns, and treatment of symptomatic individuals) at a time are sufficient for reducing the spread of COVID-19. On other hand, the government should take initiative to monitor all immigrants and ensure necessary actions such as screening and curative measures are in place to ensure the safety of individuals. Furthermore, public health education on preventive measures through various media such as television, radio stations, magazines, and posters are critical in controlling the dissemination of COVID-19 to the general public.

Conflict of Interest: No conflict of interest.

References

Adegboye OA, Adekunle AI and Gayawan E 2020 Early transmission dynamics of novel coronavirus (COVID-19) in Nigeria. *Int. J. Environ. Res. Public Health* 17(9): 3054.

Adhikari SP, Meng S, Wu YJ, Mao YP, Ye RX, Wang QZ, Sun C, Sylvia S, Rozelle S, Raat H and Zhou H 2020 Epidemiology, causes, clinical manifestation and diagnosis, prevention and control of coronavirus disease (COVID-19) during the early outbreak period: a scoping review. *Infect. Dis. Poverty* 9(1): 1-12.

Alfred H, Laurencia NM, Raymond K 2021 Modelling transmission dynamics of coronavirus with infected immigrants in Tanzania. *Afr. J. Pure Appl. Sci.* 2(2): 118-126.

Birkhoff G and Rota GC 1982 Ordinary Differential Equations, Ginn and Co, Boston.

Marouf FE 2021 The impact of COVID-19 on immigration detention. *Frontiers in Human Dynamics* 2: 599222.

Fleming W and Rishel R 1975 Deterministic and Stochastic Optimal Controls, Springer Verlag, New York.

Gwee SXW, Chua PEY, Wang MX and Pang J 2021 Impact of travel ban implementation on COVID-19 spread in Singapore, Taiwan, Hong Kong and South Korea during the early phase of the pandemic: a comparative study. *BMC Infect. Dis.* 21(1): 1-17.

Ivorra B, Ferrández MR, Vela-Pérez M and Ramos AM 2020 Mathematical modelling of the spread of the coronavirus disease 2019 (COVID-19) taking into account the undetected infections. The case of China. *Commun. Nonlinear Sci. Numer. Simul*. 88: 105303.

Jia J, Ding J, Liu S, Liao G, Li J, Duan B, Wang G and Zhang R 2020 Modeling the Control of COVID-19: Impact of policy interventions and meteorological factors. *Electron. J. Differ. Equ.* 23: 1-24.

Kassa SM, Njagarah JBH and Terefe YA 2020 Analysis of the mitigation strategies for COVID-19: From a mathematical modelling perspective. *Chaos, Solitons & Fractals* 138: 109968.

Kucharski AJ, Russell TW, Diamond C, Liu Y, Edmunds J, Funk S, Sun F, Jit M, Munday JD and Davies N 2020 Early dynamics of transmission and control of COVID-19: a mathematical modelling study. *Lancet Infect. Dis*. 20(5): 553-558.

Lee VJ, Chiew CJ and Khong WX 2020 Interrupting transmission of COVID- 19 lessons from containment efforts in Singapore. *J. Travel Med.* 27(3): 039

Lenhart S and Workman JT 2007 Optimal control applied to biological models. Chapman and Hall/CRC.

Mukandavire Z, Chiyaka C, Garira W and Musuka G 2009 Mathematical analysis of a sex-structured HIV/AIDS model with a discrete-time delay. *Nonlinear Anal.: Theory, Methods Appl.* 71(3-4): 1082-1093.

Mumbu ARJ and Hugo AK 2020 Mathematical modelling on COVID-19 transmission impacts with preventive measures: a case study of Tanzania. *J. Biol. Dyn.* 14(1): 748-766.

Rahman A and Kuddus MA 2021 Modelling the transmission dynamics of COVID-19 in six high-burden countries. *BioMed. Res. Int.* 2021.

Seidu B 2020 Optimal strategies for control of COVID-19: A mathematical perspective. *Scientifica* 2020.

Singh S, Parmar KS, Kumar J and Makkhan SJS 2020 Development of new hybrid model of discrete wavelet decomposition and autoregressive integrated moving average (ARIMA) models in application to one month forecast the casualties cases of COVID-19. *Chaos, Solitons & Fractals* 135: 109866.

Tarimo CS and Wu J 2020 The first confirmed case of COVID-19 in Tanzania: recommendations based on lesson learned from China. *Trop. Med. Health* 48(1): 1-3.

Tchoumi SY, Rwezaura H, Diagne ML, González-Parra G and Tchuenche J 2022 Impact of infective immigrants on COVID-19 dynamics. *Math. Comput. Appl.* 27(1): 11.

Van den Driessche P and Watmough J 2002 Reproduction numbers and sub-threshold endemic equilibria for compartmental models of disease transmission. *Math. Biosci*. 180(1–2): 29-48.

World Health Organization 2021 Refugees and migrants in times of COVID-19: mapping trends of public health and migration policies and practices: *Global Evidence Review on Health and Migration.*

Xing GR, Li MT, Li L and Sun GQ 2020 The Impact of population migration on the spread of COVID-19: A case study of Guangdong Province and Hunan Province in China. *Front. Phys.* 8: 488.